International Journal of Heat and Technology
Vol. 42, No. 6, December, 2024, pp. 1924-1934
Journal homepage: http://iieta.org/journals/ijht

Effect of Pyrolysis Temperature on the Properties of Biochar Derived from Melinjo Seed Shells

Ali Rahmat[1*], Annisa Saadatul Awwaliyah[2], Hidayat Hidayat[1], Ivone Wulandari Budiharto[2], Fera Arum[1], Santi Ari Respati[1], Wiwiek Dwi Susanti[1], Sukamto Sukamto[3]

[1] National Research and Innovation Agency, Jakarta 10340, Indonesia
[2] Department of Environmental Engineering and Management, IPB University, Bogor 16128, Indonesia
[3] Graduate School of Life Science, Hokkaido University, Sapporo 060-0810, Japan

Corresponding Author Email: alirahmatoffice@gmail.com

https://doi.org/10.18280/ijht.420609

Received: 23 July 2024
Revised: 16 November 2024
Accepted: 29 November 2024
Available online: 31 December 2024

Keywords:
biochar, carbon sequestration, melinjo shell, pyrolysis, soil amendment, thermal stability, waste

ABSTRACT

The potential of melinjo (Gnetum gnemon) seed shells as a source of biochar was evaluated by subjecting the biomass to pyrolysis at temperatures ranging from 300°C to 600°C. The objective was to investigate the effect of pyrolysis temperature on the yield, structural, and physicochemical properties of the resultant biochars. Pyrolysis was performed in a controlled furnace, and a comprehensive analysis of the biochar was conducted, including thermogravimetric analysis (TGA), surface morphology, Brunauer-Emmett-Teller (BET) surface area, crystallinity, functional groups, proximate and ultimate analyses, and nutrient content. The yield of biochar was observed to decrease with an increase in pyrolysis temperature, from 56.28% at 300°C to 37.03% at 600°C. Elevated pyrolysis temperatures were found to reduce the volatile matter, average pore radius, and the concentration of elements such as hydrogen (H), sulfur (S), and oxygen (O). In contrast, higher temperatures enhanced the biochar's thermal stability, specific surface area, total pore volume, crystallinity, fixed carbon content, and the concentration of nutrients such as magnesium (Mg), phosphorus (P), and nitrogen (N). Biochar produced at 600°C exhibited excellent thermal stability, with a BET surface area of 41.313 m^2g^{-1}, a total pore volume of 0.0685 cm^3g^{-1}, and a fixed carbon content of 73.32%. Notably, the biochar was rich in essential nutrients, including magnesium (4.043 mg g^{-1}), potassium (K, 3.115 mg g^{-1}), phosphorus (1.182 mg g^{-1}), and nitrogen (6.385 mg g^{-1}). The biochar's porous structure and alkaline nature are conducive to enhancing soil fertility by improving water retention, increasing nutrient availability, and buffering soil acidity. These findings suggest that melinjo seed shells, when subjected to pyrolysis at higher temperatures, could be a viable source of high-quality biochar for sustainable agricultural applications.

1. INTRODUCTION

Gnetum gnemon L., the scientific name for the melinjo plant, is indigenous to Indonesia and a member of the Gnetaceae family. Its fruits and seeds are commonly utilized as components in vegetable dishes and snacks [1]. Melinjo, a significant commodity in Indonesia, is processed into chips from its seeds [2]. In the Gnetum gnemon cracker industry, both the outer skin and endosperm of the seeds are employed to manufacture crackers; however, the hard shell is deemed waste and discarded. The positive results presented here prompt further exploration, as this aspect holds considerable potential interest, not only concerning health but also in terms of environmental sustainability by reducing bio-waste [3].

The melinjo bean is widely consumed, resulting in the generation of bean shells as waste in food industry operations [4]. In a study by Lelifajri et al. [5], melinjo shell waste was converted into carbon, highlighting its impressive potential as a carbon source. Fatimah et al. [4] demonstrated that melinjo can serve as a raw material for carbon. Similarly, Dwijayanti and Kartika [6] uncovered the significant carbon potential of this plant. They produced charcoal from melinjo shells through processes involving carbonization, chemical activation, and physical activation. The resulting charcoal comprised 87-97% carbon, with the remainder consisting of hydrogen, sulfur, oxygen, and numerous other compounds. Charcoal can be associated with biochar where the feedstock is from organic material.

Currently, research on utilizing melinjo peel as biochar and exploring its characteristics and potential in the agricultural sector remains limited. Most studies have primarily focused on converting melinjo seed shells into carbon products for dye adsorption or transforming them into briquettes.

Transforming waste materials into biochar can enhance economic value and contribute to environmental sustainability. Moreover, repurposing waste for biochar production can lower waste disposal expenses [7]. The transformation of waste into biochar serves as a method for waste management and recycling. Subsequent research endeavors should prioritize refining biochar application techniques for agricultural and

environmental benefits, alongside evaluating the carbon dynamics within biochar-enriched agricultural systems [8]. The production of biochar involves subjecting residues from trees, shrubs, grasses, or organic wastes to pyrolysis, with oxygen partially or fully excluded [9].

Biochar has diverse applications, serving as a reliable solid fuel for domestic energy needs, such as heating and meal preparation, and as a bio-adsorbent in water purification and wastewater management [10-12]. With its organic carbon content, biochar contributes to mitigating global warming [13]. Furthermore, it can be utilized in the creation of activated carbon, provided its porosity and surface characteristics are adequate [14]. The surging attention toward biochar arises from its potential in carbon capture and storage and its ability to enhance soil fertility [15]. Moreover, biochar shows promise as an additive for agricultural soils, enhancing soil amendment and agronomy [16].

The properties and behavior of biochars vary significantly, even when produced from similar feedstock and pyrolysis conditions, which means that study results may not be universally valid for all biochar types [17]. Furthermore, the properties of biochar are determined by the feedstock type and the pyrolysis method employed. Therefore, further investigation is necessary to ascertain the distinct characteristics of biochar produced from melinjo seed shells at varying pyrolysis temperatures. The outcomes of this study could offer insights into more effective strategies for utilizing melinjo seed shell waste.

2. METHODS

2.1 Biochar production

Melinjo seed shell waste is obtained from traditional markets. The shells are then washed to remove dirt and air-dried for 24 hours. Next, the melinjo seed shells are crushed with a chopper and sifted using a 10-mesh sieve. The melinjo seed shells are subsequently oven-dried at 105℃ for a duration of 24 hours. Once the drying process is complete, the sample is permitted to cool, making it suitable for use in the pyrolysis process.

In the pyrolysis process, melinjo seed shells are placed in a 100 mL porcelain cup with a lid, with approximately 80 g of material per cup. The porcelain cup is covered with its lid and wrapped in aluminum foil to minimize oxygen exposure during pyrolysis. The prepared samples (8 cups) are then loaded into a muffle furnace. The melinjo seed shells undergo pyrolysis at temperatures of 300, 400, 500, and 600℃. It takes approximately 45 minutes to reach the target pyrolysis temperature. The process is maintained for 4 hours once the temperature is stabilized. Afterward, the furnace is turned off, and the biochar is left to cool for 24 hours until it reaches room temperature. The biochar is subsequently taken from the reactor, weighed, ground, and subjected to a 60-mesh sieve. The sieved samples are then prepared for further analysis (details of the process are shown in Figure 1). This study employed a temperature range between 300 and 600℃ to evaluate the breakdown of organic materials through thermal decomposition. It is well established that thermal decomposition for most organic substances typically starts at around 300℃ [18]. Higher temperatures accelerate the decomposition rate, with 400℃ significantly increasing the release of volatile compounds and bio-oil production [19]. A temperature of 500℃ is often considered ideal for initiating pyrolysis, effectively converting organic material into simpler components [20]. At 600℃, the highest temperature tested, carbonization reaches its maximum level [18, 19]. The findings, including material characterization, aim to help farmers and other users choose the most appropriate temperature based on their equipment and the desired pyrolysis product.

Figure 1. Flowchart of melinjo seed shell biochar production

2.2 Analysis of biochar characteristics

In this research, several characteristics of biochar were examined, including biochar yield, surface morphology, TGA, Fourier Transform Infrared Spectroscopy (FTIR), specific surface area, total pore volume, average pore size, X-ray Diffraction (XRD), proximate analysis, ultimate analysis, and nutrient content. Details information can be seen in Table 1.

Table 1. The instrument used for biochar characterization

No.	Instrument	Characteristics of Biochar
1	Thermo Scientific Quattro S FESEM	Surface morphology
2	NETZSCH STA 449F3 Simultaneous Thermal Analyzer	TGA
3	FTIR with the PerkinElmer Spectrum	Functional group
4	X-Ray Diffraction 7000 Shimadzu	Crystal condition
5	American Standard Testing Method (ASTM) D3173, D3174 D3175 utilizing furnace	Proximate analysis
6	ASTM D3573, D4239 utilizing CHN analyzer Leco CHN 628	Ultimate analysis
7	Atomic Absorption Spectrometer (AAS) type Thermo Scientific iCE 3000	Kalium (K), Magnesiaum (Mg)
8	Spektrofotometer uv-vis	Nitrogen (N) and Phosphor (P)

3. RESULTS AND DISCUSSION

3.1 Biochar yield of melinjo seed shell biochar

Melinjo seed shells were transformed into biochar by pyrolysis at various temperatures of 300, 400, 500, and 600°C. The pyrolysis temperature had a significant impact on the yield of biochar, which varied between 37.03% and 56.28%, as shown in Figure 2. Increased pyrolysis temperatures led to a reduction in biochar yield, probably attributable to the more thorough decomposition of lignocellulosic substances at higher temperatures. Lignocellulose comprises three primary polymers: cellulose, hemicellulose, and lignin [21], each with distinct thermal decomposition profiles [22].

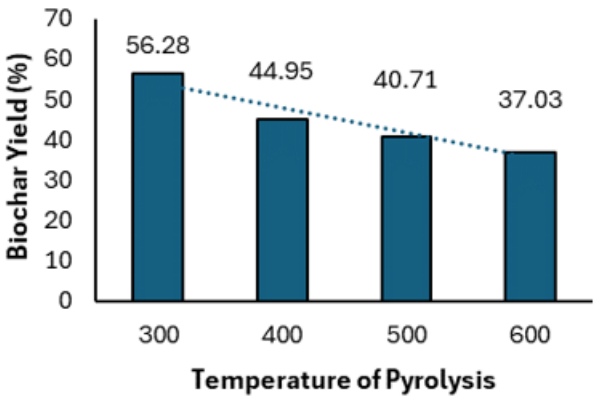

Figure 2. Melinjo seed shell biochar yield

TGA revealed that hemicellulose undergoes maximum degradation between 185 and 325°C, cellulose between 270 and 400°C, and lignin between 200 and 500°C [23]. Consequently, elevated temperatures result in increased breakdown of these components, thereby diminishing the production of biochar.

3.2 TGA of biochar

Figure 3 indicates the percentage of fraction mass loss and degradation behavior of the melinjo seed shell biochar in relation to temperature. Figure 3 shows the percentage differences in mass loss at each stage, with intervals of 100°C.

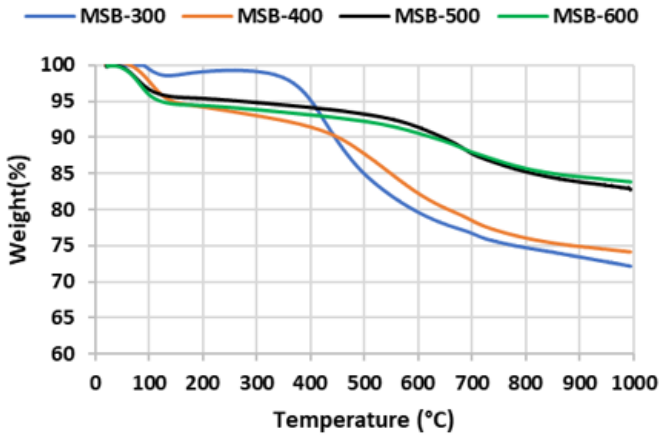

Figure 3. TGA analysis of biochar from melinjo seed shell biochar (MSB)

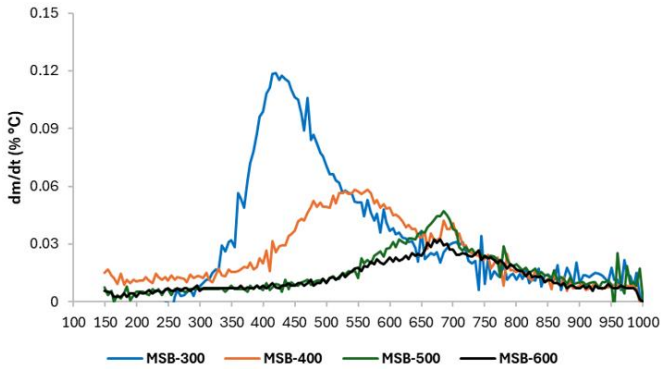

Figure 4. Differential thermogravimetry analysis of biochar

Figure 3 illustrates the initial mass loss resulting from moisture evaporation from the biochar [24, 25]. A mass loss of about 5-6% was recorded at 200°C. The response of biochar to varying temperatures exhibited notable variation. For the MSB-300 sample, mass loss began at 335°C, accelerated at 400°C, and reached its peak at 420°C (Figure 4). Although mass loss continued at higher temperatures, the rate of reduction became less pronounced. In the case of MSB-400, mass loss increased with temperature, with the most significant loss occurring at 565°C. Conversely, MSB-500 and MSB-600 displayed peak mass losses at 685°C and 670°C, respectively.

The thermogravimetric and differential thermogravimetric results obtained align with the observations made by Zhao et al. [26], confirming that the biochar samples had undergone prior thermal treatment before analysis. This suggests that the biochars were thermally stable below their respective production temperatures. As shown in Figure 4, each biochar sample exhibited a distinct peak on the DTG curve within the temperature range of the production temperature and 1000°C. Secondary pyrolysis reactions, which are typically detectable at temperatures higher than the primary decomposition temperature of biochar, contributed to the broader weight loss range [25]. This weight loss can be attributed to the breakdown

and degradation of organic matter within the biochar [27]. The maximum mass loss for MSB-300, MSB-400, MSB-500, and MSB-600 occurred at approximately 420°C, 565°C, 685°C, and 670°C, respectively (Figure 4). These results indicate that higher pyrolysis temperatures enhance the thermal resistance of biochar, in line with previous studies [28].

Sun et al. [27] demonstrated that biochar produced at lower temperatures tends to be less thermally stable compared to biochar produced at higher temperatures due to incomplete carbonization. The degree of mass loss is dramatically affected by the biochar production technique. In the case of MSB-300, the greatest mass loss was observed because it was produced at 300°C and still contained substantial amounts of cellulose, hemicellulose, and lignin, which were only partially degraded. As a result, when the analysis temperature exceeds 300°C, many of these substances evaporate. According to Sonobe et al. [29], the degradation of cellulose is the primary cause of significant mass loss. Zhang et al. [30] identified 340°C as the threshold temperature for the breakdown of crystalline cellulose. Additionally, the peak mass loss for MSB-300 occurs at 420°C, consistent with findings by Ma et al. [23], which indicate significant lignin decomposition at this temperature.

3.3 Surface morphology of biochar

The morphology of melinjo seed shell biochar is a crucial physical property, significantly influenced by pyrolysis temperature. Scanning Electron Microscopy (SEM) at 1000x magnification was utilized to analyze the differences in surface morphology of biochar produced at various pyrolysis temperatures. The pyrolysis process induces changes in surface patterns and pore sizes in biochar, which are essential for its effectiveness as an absorbent material [31]. Figure 4 depicts the shape of melinjo seed shell biochar at pyrolysis temperatures of 300 to 600°C.

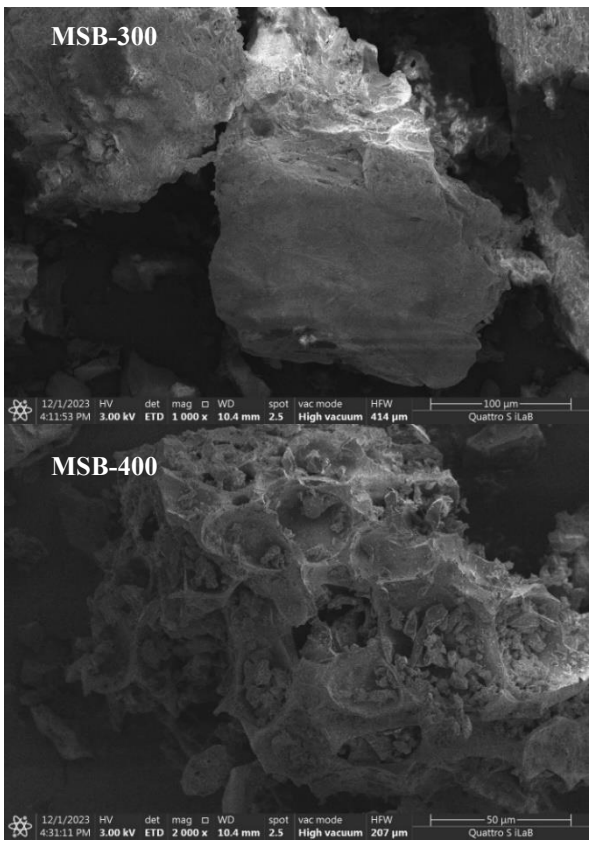

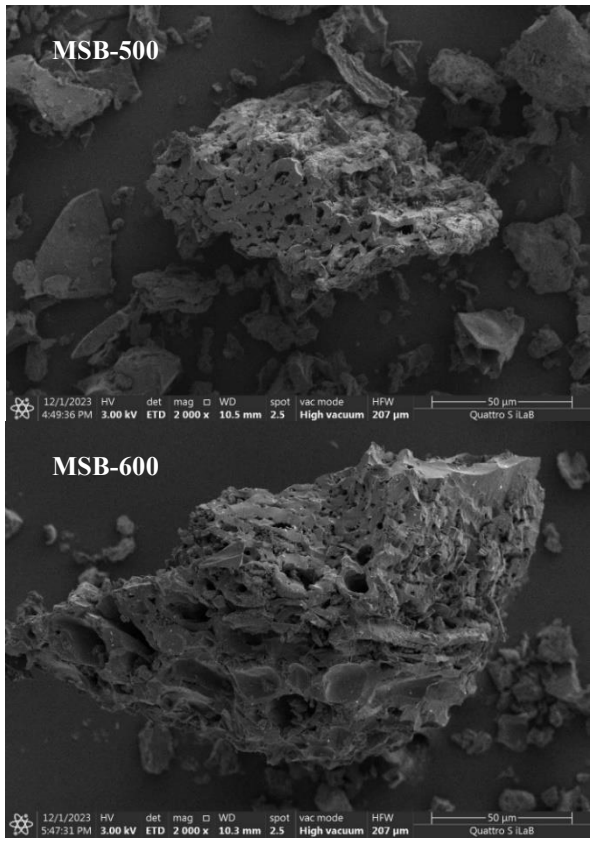

Figure 5. Surface morphology of melinjo seed shell biochar

From Figure 5, it is evident that biochar pyrolyzed at 300°C has not yet developed pores. This is consistent with Claoston et al. [32], who noted that incomplete pore formation is due to tissue that has not undergone devolatilization. At 400°C, the melinjo seed shell biochar begins to form pores, and at 500°C, it exhibits a morphology with interconnected pores. Higher pyrolysis temperatures facilitate the release of volatile organic compounds [33]. Hemicellulose and cellulose volatilize at temperatures below 400°C, whereas lignin volatilizes at temperatures above 400°C [23]. The absence of pore formation at 300°C is due to the presence of a significant amount of undecomposed volatile material. This is corroborated by Figure 2, which shows a marked decrease in the biochar mass at 400°C during TGA. The evaporation of these organic materials leads to the appearance of pores on the biochar surface. The surface morphology of biochar pyrolyzed at 600°C shows more distinct pores, attributed to the higher pyrolysis temperature.

3.4 BET surface area value, total pore volume, and average pore radius of biochar

The influence of temperature during pyrolysis on melinjo seed shell biochar is detailed in Table 2. The BET specific surface area of the biochar ranges from 0 to 41.313 m^2g^{-1}, with the highest value of 41.313 m^2g^{-1} observed at 600°C, which is ten times greater than the BET surface area at 400°C. This indicates that increasing pyrolysis temperature results in a larger BET surface area for the melinjo seed shell biochar.

At higher pyrolysis temperatures, the rapid emission of volatile compounds leads to more uniformly arranged pores and the formation of micropores within larger pores, thereby increasing the BET surface area [34]. Elnour et al. [35] also support this, noting that the loss of volatile substances plays a

role in the enhancement of the BET specific surface area of biochar. This phenomenon is evident in the biochar's surface morphology (Figure 5). Increased pyrolysis temperatures result in the formation of additional pores.

Table 2. BET surface area value, total pore volume, and average pore radius of melinjo seed shell biochar

Biochar	BET Surface Area (m^2g^{-1})	Total Pore Volume ($cc\ g^{-1}$)	Average Pore Radius (Å)
MSB 300			
MSB 400	4,097	0,0295	144,177
MSB 500	25,132	0,0611	48,6632
MSB 600	41,313	0,0685	33,1623

MSB = Melinjo seed shall biochar

The total pore volume of the biochar also shows an increasing trend alongside the rise in BET surface area at higher pyrolysis temperatures. Mukome et al. [36] observed that elevated temperatures facilitate the formation of pores in biochar, leading to the highest total pore volume of 0.0685 cc/g for melinjo seed shell biochar at 600°C. There is an observed increase in both the BET surface area and total pore volume, while the average pore radius decreases with rising pyrolysis temperatures. The lowest average pore radius is observed in melinjo seed shell biochar at 600°C, which is attributed to the conversion of a significant number of macropores into micropores.

3.5 XRD of biochar

Figure 6 presents the XRD pattern, which highlights a broad diffraction peak within the 2-theta angle range of 18°-28°. This broadening is indicative of the amorphous structure of the C (002) plane in biochar, resulting from the alignment of aromatic compounds that undergo partial carbonization as the pyrolysis temperature increases. A notable peak at 600°C, located at approximately 43.4°, corresponds to the crystal plane index C (100), signifying the condensed aromatic carbonization plane and reflecting the degree of crystallization of carbon in the biochar sample [37].

The crystallinity percentages of biochar produced at 300°C, 400°C, 500°C, and 600°C are 18.51%, 59.55%, 98.45%, and 41.91%, respectively. Several factors may contribute to the reduction in biochar crystallinity, including the formation of amorphous structures, the creation of complex compounds, excessive heating or decomposition, the presence of impurities or minerals, and the interplay between crystalline and amorphous phases [38-40]. The data indicate that at 300°C, a broader amorphous peak is observed compared to other temperatures, which can be attributed to the presence of oxygenated and aliphatic functional groups. With increasing temperature from 300°C to 500°C, the aromatic and cyclic structures of the material become more pronounced, while a significant amorphous component remains present [41].

Biochar with low crystallinity demonstrates enhanced adsorption capacity due to the increased availability of active functional groups that arise from its more disordered crystal structure. In contrast, crystalline biochar exhibits superior chemical stability. Amorphous biochar, on the other hand, provides a greater number of reactive sites, facilitating environmental chemical interactions, including adsorption, catalysis [42], and interactions with dyes, heavy metals, and other organic compounds [43], as shown in studies examining crystal violet dye adsorption using biochar [44].

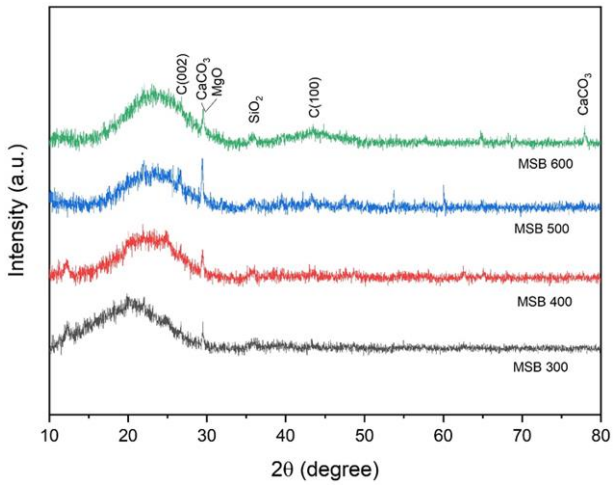

Figure 6. XRD of melinjo seed shell biochar

The research data analyzed by Aftab et al. [45] revealed diffraction peaks at 44.67° and 78.69°, corresponding to the presence of $CaCO_3$ (calcite), as indicated by JCPDS Card no. 05-0586. The peaks in the CaO sample, matching JCPDS Card no. 28-0775, appeared at 24.28°, 29.52°, 31.28°, and 35.61°. MgO was identified at angles 29.52°, 40.62°, 60.33°, 65.73°, and 75.66°, consistent with JCPDS Card no. 30-0794. Additionally, peaks corresponding to SiO_2, according to JCPDS Card no. 80-2157, were detected at 35.61°, 42.5°, 46.02°, 50.4°, and 70.65°.

Biochar is composed of a variety of inorganic constituents, including metal carbonates, sulfates, phosphates, silicates, and chlorides. Research indicates a direct relationship between biochar alkalinity and the presence of $CaCO_3$ and MgO. When applied to acidic soils, basic minerals such as $CaCO_3$ and MgO interact with reactive soil components, such as protons, thereby reducing soil acidity [46].

3.6 Functional group of biochar

The FTIR spectrum of MSB biochar, generated at pyrolysis temperatures between 300°C and 600°C, is illustrated in Figure 7. The surface of biochar exhibits various oxygen-containing functional groups, such as -COOH, -OH, aromatic compounds, lipids, and alkanes. The absorption peaks observed at approximately 3200 and 3400 cm^{-1} correspond to the stretching vibrations of the -OH group. The most intense vibration of the $-CH_2$ group in cyclic or naphthenic hydrocarbons typically appears around 2900 cm^{-1}. However, this peak is absent in the MSB spectra within the 300°C to 600°C temperature range due to the gradual breakdown of these groups at higher temperatures [38]. The findings suggest that an increase in pyrolysis temperature results in a reduction in alkane groups [47].

The region between 1567–1371 cm^{-1} in Figure 6 contains several asymmetric peaks, with the most significant peak reflecting a high degree of disorder or defects typical of amorphous carbon at 600°C. The peak at 1567 cm^{-1} corresponds to C=C bending vibrations [48], while the one near 1371 cm^{-1} is associated with C-H bond strain. All samples show the presence of benzene ring compounds on the biochar surface, confirming that MSB forms an aromatic structure during carbonization [20]. The study indicates that elevated pyrolysis temperatures enhance the formation of aromatic compounds, in contrast to biochar produced at or below 300°C. As the temperature rises, the extent of aromatization also

increases [48].

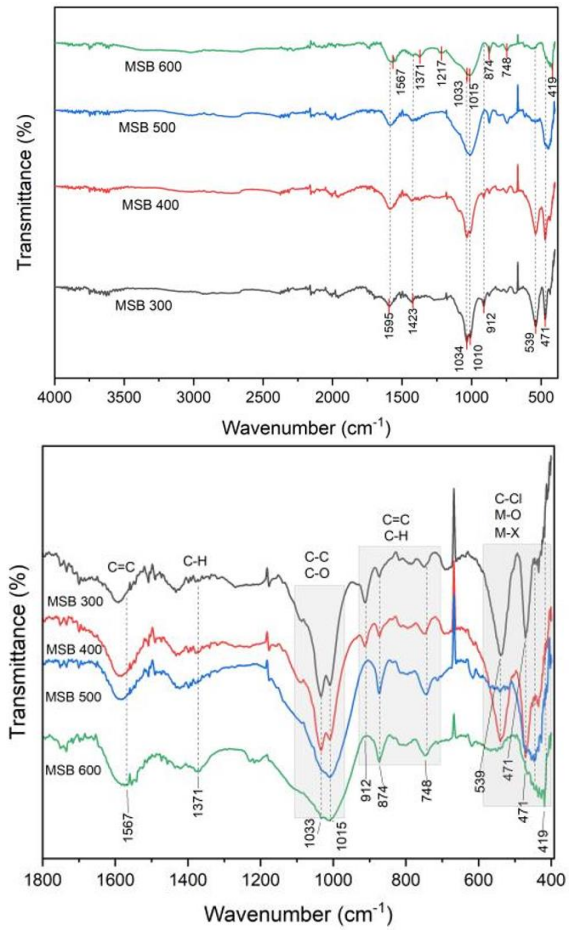

Figure 7. Spektrum FTIR melinjo seed shell biochar 300℃-600℃

At 300℃, the peaks observed at 1033 cm^{-1} and 1010 cm^{-1} shift and merge into a single peak at 1015 cm^{-1}, indicating the presence of C-C and C-O groups [49]. Peaks detected at 874 cm^{-1} and 748 cm^{-1} suggest the absorption of C=C bending vibrations within the aromatic ring. The band at 874 cm^{-1} in both biochars is related to the elongation of C=O carbonate groups in calcite [50]. The peaks at 748 cm^{-1} and 418 cm^{-1} in MSB are due to the asymmetric bending vibrations of Si-O-Si and the symmetric stretching of Si-O, respectively [51]. At 600℃, the crystalline MgO peak at 539 cm^{-1} [52] shifts to 471 cm^{-1}, indicating a transition to a more amorphous state. Additionally, $CaCO_3$ decomposes into CaO and CO_2 gas [53]. The signal at 418 cm^{-1} corresponds to the C-Cl bond [54].

3.7 Proximate analysis and ultimate analysis of biochar

Proximate analysis was conducted to assess the moisture content, ash content, volatile matter, and fixed carbon in the melinjo seed shell biochar, as detailed in Table 3. The moisture content in the biochar samples produced at temperatures ranging from 300℃ to 600℃ exhibited minimal variation, with values between 4.77% and 5.07%. The highest moisture content of 5.07% was found in the biochar produced at 600℃. This can be attributed to the extended carbonization process, which increases the porosity of the biochar, leading to greater exposure to air. As a result, the biochar's hygroscopic nature facilitates higher water absorption, consistent with the observed rise in total pore volume at this temperature [55].

Table 3. Proximate analysis data of melinjo seed shells biochar

Biochar	Moisture Content	Ash Content	Volatile Matter	Fixed Carbon
	(%)			
MSB 300	4.77	17.88	41.71	40.41
MSB 400	5.24	11.78	23.90	64.32
MSB 500	4.27	19.48	14.15	63.54
MSB 600	5.07	18.54	9.15	73.32

The ash content of melinjo seed shell biochar reached its peak at 19.48% at 500℃, while the lowest ash content of 11.78% was observed at 400℃. Ash represents the inorganic fraction that remains non-volatile and non-degradable through combustion. The increased ash content aligns with the decomposition of the lignin at higher pyrolysis temperatures, as lignin contains more ash [56]. The decrease in ash content at 600℃ may be due to the release and further oxidation or decomposition of ash [32].

Melinjo seed shell biochar produced at 600℃ exhibited the lowest volatile matter content at 9.15%, whereas the biochar produced at the lowest temperature had the highest volatile matter content at 41.71%. This reduction is due to the thermal decomposition of cellulose and lignin, as well as the degradation of cellulose, hemicellulose fractions, and non-carbon combustible biomass components during pyrolysis [32]. The greater loss of volatile matter at elevated temperatures leads to a more developed pore structure and increased carbon stability [57].

The fixed carbon content in melinjo seed shell biochar augmented at elevated pyrolysis temperatures. Biochar generated at 300℃ had the lowest fixed carbon content at 40.41%, whereas biochar created at 600℃ demonstrated the highest fixed carbon content at 73.32%. The rise in fixed carbon content is ascribed to the decrease in volatile matter concentration in the biochar.

Table 4. Results of ultimate analysis of melinjo seed shell biochar

Biochar	C	H	N	S	O
	%				
MSB 300	60.69	4.14	0.97	0.23	16.09
MSB 400	70.04	3.27	0.71	0.17	14.03
MSB 500	69.88	2.62	0.74	0.18	7.10
MSB 600	74.08	1.92	0.64	0.16	4.66

Ultimate analysis was performed to quantify the content of carbon (C), hydrogen (H), nitrogen (N), sulfur (S), and oxygen (O) in melinjo shell biochar. Among these, carbon (C) is the most abundant nutrient element in the biochar. The biochar pyrolyzed at 600℃ exhibited the highest carbon content at 74.08% (Table 4). The increase in carbon content can be attributed to the breakdown and elimination of most non-carbon elements during the pyrolysis process [58].

As shown in Table 3, the contents of hydrogen (H), nitrogen (N), sulfur (S), and oxygen (O) decrease with higher pyrolysis temperatures, in agreement with the observations of Adekanye et al. [59]. The reduction in oxygen content is attributed to the release of CO and CO_2 during pyrolysis [60]. The decrease in hydrogen content results from the breakdown of oxygenated

functional groups and the emission of hydrogen-rich gases with lower molecular weights. Nitrogen and sulfur are eliminated as they transition to the gas phase during pyrolysis, forming N_2 and various sulfur compounds [61].

3.8 Nutrient content of biochar

Biochar typically contains essential macronutrients such as magnesium (Mg), potassium (K), phosphorus (P), and nitrogen (N), which are crucial for plant growth. The magnesium content ranges from 1.079 to 4.043 mg g^{-1}, potassium from 3.115 to 5.088 mg g^{-1}, phosphorus from 1.013 to 1.309 mg g^{-1}, and nitrogen from 5.302 to 6.385 mg g^{-1}. According to the analysis, biochar produced at a pyrolysis temperature of 600°C shows the highest Mg and total N content. Notably, the magnesium content increases with rising pyrolysis temperatures.

The Mg content in melinjo seed shell biochar increases with higher pyrolysis temperatures, rising from 1.358 mg g^{-1} at 500°C to 4.043 mg g^{-1} at 600°C. This increase is attributed to the evaporation of organic compounds from the biomass, which results in the concentration of minerals [62]. Similarly, the K content rises from 3.873 mg g^{-1} at 300°C to 5.088 mg g^{-1} at 500°C but decreases to 3.115 mg g^{-1} at 600°C, likely due to the volatilization of KCl and the decomposition of potassium complexes and graphite-K layers [63]. The K concentration in melinjo shell biochar is comparable to that of biochar derived from hardwood oak, which has K concentrations of 1.3, 3.8, and 4.5 mg g^{-1} at pyrolysis temperatures of 200°C, 400°C, and 600°C, respectively [64]. The P content in melinjo shell biochar increases from 1.013 mg g^{-1} at 300°C to 1.309 mg g^{-1} at 500°C but declines to 1.182 mg g^{-1} at 600°C due to the volatilization of P at elevated temperatures [65]. Compared to hardwood oak biochar, melinjo shell biochar exhibits higher P concentrations, with values of 0.3, 0.6, and 0.6 mg g^{-1} at pyrolysis temperatures of 200°C, 400°C, and 600°C, respectively [64]. The N content in melinjo shell biochar fluctuates with pyrolysis temperature, decreasing between 400°C and 500°C due to the volatilization of N in the uncondensed gas mixture [66], but increasing to 6.385 mg g^{-1} at 600°C. When compared to soybean straw biochar, the N concentration in melinjo seed shell biochar is lower at 300°C but higher at 500°C and 700°C, with concentrations of 12.7, 3.7, and 1 mg g^{-1}, respectively [67].

While biochar is not an immediate source of nutrients like conventional fertilizers, it offers long-term improvements to soil conditions when used as a soil amendment. As shown in Table 4, biochar is primarily composed of carbon, with melinjo seed shell biochar containing 60-74% carbon. When incorporated into soil, biochar's carbon remains more stable compared to non-pyrolyzed carbon due to the thermal degradation it undergoes during production. As a stable form of carbon derived from biomass waste materials, biochar can remain in soil for several decades, thus reducing or delaying carbon emissions from biomass [68, 69]. Furthermore, biochar has the potential to reduce greenhouse gas emissions from soils and foster carbon sequestration in vegetation by improving soil structure and supporting microbial activity [70]. Therefore, biochar is viewed as a valuable material for carbon sequestration and advancing carbon neutrality in soils [71].

In addition to its role in carbon sequestration, biochar can enhance soil fertility. Melinjo shell biochar contains essential macronutrients such as Mg, K, P, and N. When applied to soil, these nutrients can improve soil fertility, providing plants with essential nutrients. Macronutrients like Mg and K exist in cationic forms such as Mg^{2+}, K^{+}, and possibly other cations like Ca^{2+} or Na^{+}, which help increase soil pH (a liming effect) and improve soil's cation exchange capacity [72], thereby enhancing nutrient availability for plants [73].

The highest values of surface area and total pore volume observed at 600°C clearly demonstrate the effectiveness of the pyrolysis process for melinjo seed shells. An increased BET surface area in melinjo seed shell biochar is essential for improving soil properties [16]. The surface area also plays a role in determining the availability of surface charges, which directly affects the cation exchange capacity [74]. Ghosh and Maiti [75] observed that the extensive porosity in biochar provides a favorable environment for microbial activity and enzyme exchange. Porosity and the interconnectivity of pores are critical factors affecting the biochar's ability to retain water. Additionally, as shown in Table 5, MSB-600 biochar contains relatively high nutrient levels compared to other biochars, which further enhances its potential for soil nutrient retention.

Table 5. Nutrient content of Mg, K, P, and N of melinjo seed shells biochar

Biochar	Total Mg	Total K	Total P	Total N
	mg g^{-1}			
MSB 300	1.079	3.873	1.013	5.606
MSB 400	1.180	4.311	1.254	5.896
MSB 500	1.361	5.088	1.309	5.302
MSB 600	4.043	3.115	1.182	6.385

4. CONCLUSIONS

In this study, it was demonstrated that pyrolysis temperature significantly influences the physicochemical characteristics of melinjo seed shell biochar. Higher pyrolysis temperatures resulted in reduced biochar yield and volatile matter while enhancing critical attributes such as thermal stability, surface area, pore volume, and nutrient content (Mg, P, N). Biochar generated at 600°C demonstrated enhanced thermal stability, elevated alkalinity, and a rich nutrient profile, positioning it as a viable option for soil amendment. Its potential to improve soil structure, increase nutrient retention, and support carbon sequestration emphasizes its relevance for sustainable agricultural practices. However, further studies are required to assess its effect on soil quality and its effectiveness in carbon sequestration.

ACKNOWLEDGMENT

We extend our deepest gratitude to the Organisasi Riset Nanoteknologi dan Material-BRIN for its support of this research through the program (Grant No.: 20/III.10/HK/2024) and Riset dan Inovasi untuk Indonesia Maju (RIIM), Direktorat Pendanaan Riset dan Inovasi (Grant No.: NOMOR 82/II.7/HK/2022).

REFERENCES

[1] Bhat, R., Yahya, N.B. (2014). Evaluating belinjau (Gnetum gnemon L.) seed flour quality as a base for development of novel food products and food formulations. Food Chemistry, 156: 42-49.

https://doi.org/10.1016/j.foodchem.2014.01.063
[2] Siswoyo, T.A. (2004). Physicochemical characteristics of mlinjo (Gnetum gnemon) starch-lipid. Journal Ilmu Dasar, 5(2): 97-102.
[3] Saraswaty, V., Ketut Adnyana, I., Pudjiraharti, S., Mozef, T., Insanu, M., Kurniati, N.F., Rachmawati, H. (2017). Fractionation using adsorptive macroporous resin HPD-600 enhances antioxidant activity of Gnetum gnemon L. seed hard shell extract. Journal of Food Science and Technology, 54: 3349-3357. https://doi.org/10.1007/s13197-017-2793-3
[4] Fatimah, I., Yahya, A., Sasti, R.A.T. (2017). Preparation of sodium dodecyl sulphate-functionalized activated carbon from Gnetum gnemon shell for dye adsorption. AIP Conference Proceedings, 1823: 020125. https://doi.org/10.1063/1.4978198
[5] Lelifajri, R., Rahmi, Supriatno, Susilawati. (2021). Preparation of activated carbon from Gnetum gnemon shell waste by furnace-NaCl activation for methylene blue adsorption. Journal of Physics: Conference Series, 1940: 012040. https://doi.org/10.1088/1742-6596/1940/1/012040
[6] Dwijayanti, A., Kartika, S. (2020). Characteristics of activated carbon from melinjo shells composed of TiO_2 nanoparticles. Journal of Physics: Conference Series, 1477: 052012. https://doi.org/10.1088/1742-6596/1477/5/052012
[7] Tsai, W.T., Lee, M.K., Chang, Y.M. (2007). Fast pyrolysis of rice husk: Product yields and compositions. Bioresource Technology, 98(1): 22-28. https://doi.org/10.1016/j.biortech.2005.12.005
[8] Al-Wabel, M.I., Al-Omran, A., El-Naggar, A.H., Nadeem, M., Usman, A.R. (2013). Pyrolysis temperature induced changes in characteristics and chemical composition of biochar produced from conocarpus wastes. Bioresource Technology, 131: 374-379. https://doi.org/10.1016/j.biortech.2012.12.165
[9] Siengchum, T., Isenberg, M., Chuang, S.S. (2013). Fast pyrolysis of coconut biomass–An FTIR study. Fuel, 105: 559-565. https://doi.org/10.1016/j.fuel.2012.09.039
[10] Lee, X.J., Lee, L.Y., Gan, S., Thangalazhy-Gopakumar, S., Ng, H.K. (2017) Biochar potential evaluation of palm oil wastes through slow pyrolysis: thermochemical characterization and pyrolytic kinetic studies. Bioresource Technology, 236: 155e163. https://doi.org/10.1016/j.biortech.2017.03.105
[11] Walanda, D.K., Anshary, A., Napitupulu, M., Walanda, R.M. (2022). The utilization of corn stalks as biochar to adsorb BOD and COD in hospital wastewater. International Journal of Design and Nature and Ecodynamics, 17(1): 113-118. https://doi.org/10.18280/ijdne.170114
[12] Malik, A., Napitupulu, M., Napitupulu, N.D., Walanda, D.K., Anshary, A. (2023). Utilization of Tropical Forest cacao dried leaves for environment improvement. International Journal of Design and Nature and Ecodynamics, 18(2): 457-463. https://doi.org/10.18280/ijdne.180225
[13] Lehmann, J., Rillig, M.C., Thies, J., Masiello, C.A., Hockaday, W.C., Crowley, D. (2011). Biochar effects on soil biota – a review. Soil Biology and Biochemistry. 43: 1812-1836. https://doi.org/10.1016/j.soilbio.2011.04.022
[14] Demirbas, A., Pehlivan, E., Altun, T. (2006). Potential evolution of Turkish agricultural residues as bio-gas, bio-char and bio-oil sources. International Journal of Hydrogen Energy, 31: 613-620. https://doi.org/10.1016/j.ijhydene.2005.06.003
[15] Hossain, M.K., Strezov, V., Chan, K.Y., Ziolkowski, A., Nelson, P.F. (2011). Influence of pyrolysis temperature on production and nutrient properties of wastewater sludge biochar. Journal of Environmental Management, 92: 223-228. https://doi.org/10.1016/j.jenvman.2010.09.008
[16] Shaaban, A., Se, S.M., Dimin, M.F., Juoi, J.M., Husin, M.H.M., Mitan, N.M.M. (2014). Influence of heating temperature and holding time on biochars derived from rubber wood sawdust via slow pyrolysis. Journal of Analytical and Applied Pyrolysis, 107: 31-39. https://doi.org/10.1016/j.jaap.2014.01.021
[17] Chintala, R., Mollinedo, J., Schumacher, T.E., Malo, D.D., Julson, J.L. (2014). Effect of biochar on chemical properties of acidic soil. Archives of Agronomy and Soil Science, 60(3): 393-404. https://doi.org/10.1080/03650340.2013.789870
[18] Egbosiuba, T.C. (2022). Biochar and bio-oil fuel properties from nickel nanoparticles assisted pyrolysis of cassava peel. Heliyon, 8(8): e10114. https://doi.org/10.1016/j.heliyon.2022.e10114
[19] Raza, S., Zamanian, K., Ullah, S., Kuzyakov, Y., Virto, I., Zhou, J. (2021). Inorganic carbon losses by soil acidification jeopardize global efforts on carbon sequestration and climate change mitigation. Journal of Cleaner Production, 315: 128036. https://doi.org/10.1016/j.jclepro.2021.128036
[20] Chatterjee, R., Sajjadi, B., Chen, W., Mattern, D.L., Hammer, N., Raman, V., Dorris, A. (2020). Effect of pyrolysis temperature on physicochemical properties and acoustic-based amination of biochar for efficient CO_2 adsorption. Frontiers in Energy Research, 8: 85. https://doi.org/10.3389/fenrg.2020.00085
[21] Sahay, S. (2022). Handbook of Biofuels. London: Academic Press.
[22] Wijitkosum, S., Sriburi, T. (2023). Aromaticity, polarity, and longevity of biochar derived from disposable bamboo chopsticks waste for environmental application. Heliyon, 9(9): 1-8. https://doi.org/10.1016/j.heliyon.2023.e19831
[23] Ma, Z., Chen, D., Gu, J., Bao, B., Zhang, Q. (2015). Determination of pyrolysis characteristics and kinetics of palm kernel shell using TGA-FTIR and model-free integral methods. Energy Conversion Management, 89: 251-259. https://doi.org/10.1016/j.enconman.2014.09.074
[24] Liu, X., Yu, W. (2006) Evaluating the thermal stability of high performance fibers by TGA. Journal of Applied Polymer Science, 99: 937-944. https://doi.org/10.1002/app.22305
[25] Santos, L.B., Striebeck, M.V., Crespi, M.S., Ribeiro, C.A., De Julio, M. (2015). Characterization of biochar of pine pellet. Journal of Thermal Analysis and Calorimetry, 122: 21-32. https://doi.org/10.1007/s10973-015-4740-8
[26] Zhao, S.X., Ta, N., Wang, X.D. (2017). Effect of temperature on the structural and physicochemical properties of biochar with apple tree branches as feedstock material. Energies, 10(9): 1293. https://doi.org/10.3390/en10091293
[27] Sun, Y.N., Gao, B., Yao, Y., Fang, J.N., Zhang, M., Zhou,

Y.M., Chen, H., Yang, L.Y. (2014). Effects of feedstock type, production method, and pyrolysis temperature on biochar and hydrochar properties. Chemical Engineering Journal, 240: 574-578. https://doi.org/10.1016/j.cej.2013.10.081

[28] Bruun, E.W., Hauggaard-Nielsen, H., Ibrahim, N., Egsgaard, H., Ambus, P., Jensen, P.A., Dam-Johansen, K. (2011). Influence of fast pyrolysis temperature on biochar labile fraction and short-term carbon loss in a loamy soil. Biomass and Bioenergy, 35(3): 1182-1189. https://doi.org/10.1016/j.biombioe.2010.12.008

[29] Sonobe, T., Pipatmanomai, S., Worasuwannarak, N. (2006). Pyrolysis characteristics of Thai-agricultural residues of rice straw, rice husk, and corncob by TG-MS technique and kinetic analysis. In Proceedings of the 2nd Joint International Conference on "Sustainable Energy and Environment (SEE'06), pp. 21-23

[30] Zhang, T., Jin, J., Yang, S., Hu, D., Li, G., Jiang, J. (2009). Synthesis and characterization of fluorinated PBO with high thermal stability and low dielectric constant. Journal of Macromolecular Science, Part B, 48(6): 1114-1124. https://doi.org/10.1080/00222340903041244

[31] Gai, X., Wang, H., Liu, J., Zhai, L., Liu, S., Ren, T., Liu, H. (2014). Effects of feedstock and pyrolysis temperature on biochar adsorption of ammonium and nitrate. PloS One, 9(12): e113888. https://doi.org/10.1371/journal.pone.0113888

[32] Claoston, N., Samsuri, A., Ahmad Husni, M., Mohd Amran, M. (2014). Effects of pyrolysis temperature on the physicochemical properties of empty fruit bunch and rice husk biochars. Waste Management and Research, 32(4): 331-339. https://doi.org/10.1177/0734242X14525822

[33] Batista, E.M., Shultz, J., Matos, T.T., Fornari, M.R., Ferreira, T.M., Szpoganicz, B., Freitas, R.A., Mangrich, A.S. (2018). Effect of surface and porosity of biochar on water holding capacity aiming indirectly at preservation of the amazon biome. Scientific Reports, 8(1): 10677. https://doi.org/10.1038/s41598-018-28794-z

[34] Zhao, B., O'Connor, D., Zhang, J., Peng, T., Shen, Z., Tsang, D.C.W., Hou, D. (2018). Effect of pyrolysis temperature, heating rate, and residence time on rapeseed stem derived biochar. Journal of Cleaner Production, 174: 977-987. https://doi.org/10.1016/j.jclepro.2017.11.013

[35] Elnour, A.Y., Alghyamah, A.A., Shaikh, H.M., Poulose, A.M., Al-Zahrani, S.M., Anis, A., Al-Wabwl, M.O. (2019). Effect of pyrolysis temperature on biochar microstructural evolution, physicochemical characteristics, and its influence on biochar/polypropylene composites. Applied Sciences, 9(6): 1149. https://doi.org/10.3390/app9061149

[36] Mukome, F.N.D., Zhang, X., Silva, L.C.R., Six, J., Parikh, S.J. (2013). Use of chemical and physical characteristics to investigate trends in biochar feedstocks. Journal of Agricultural and Food Chemistry, 61(9): 2196-2204. https://doi.org/10.1021/jf3049142

[37] Mohan, D., Abhishek, K., Sarswat, A., Patel, M., Singh, P., Pittman, C.U. (2018). Biochar production and applications in soil fertility and carbon sequestration-a sustainable solution to crop-residue burning in India. RSC Advances, 8(1): 508-520. https://doi.org/10.1039/c7ra10353k

[38] Roshan, A., Ghosh, D., Maiti, S.K. (2023). How temperature affects biochar properties for application in coal mine spoils? A meta-analysis. Carbon Research, 2(1): 1-17. https://doi.org/10.1007/s44246-022-00033-1

[39] Tomczyk, A., Sokołowska, Z., Boguta, P. (2020). Biochar physicochemical properties: Pyrolysis temperature and feedstock kind effects. Reviews in Environmental Science and Bio/Technology, 19(1): 191-215. https://doi.org/10.1007/s11157-020-09523-3

[40] Armah, E.K., Chetty, M., Adedeji, J.A., Estrice, D.E., Mutsvene, B., Singh, N., Tshemese, Z. (2023). Biochar: production, application and the future. In Biochar-Productive Technologies, Properties and Applications. IntechOpen. https://doi.org/10.5772/intechopen.105070

[41] Tusar, H.M., Uddin, M.K., Mia, S., Suhi, A.A., Wahid, S.B.A., Kasim, S., Sairi, N.A., Alam, Z., Anwar, F. (2023). Biochar-acid soil interactions-a review. Sustainability, 15(18): 13366. https://doi.org/10.3390/su151813366

[42] Sun, P., Hui, C., Azim Khan, R., Du, J., Zhang, Q., Zhao, Y.H. (2015). Efficient removal of crystal violet using Fe3O4-coated biochar: The role of the Fe_3O_4 nanoparticles and modeling study their adsorption behavior. Scientific Reports, 5(1): 12638. https://doi.org/10.1038/srep12638

[43] Tan, X., Liu, Y., Gu, Y., Liu, S., Zeng, G., Cai, X., Hu, X., Wang, H., Liu, S., Jiang, L. (2016). Biochar pyrolyzed from MgAl-layered double hydroxides pre-coated ramie biomass (Boehmeria nivea (L.) Gaud.): Characterization and application for crystal violet removal. Journal of Environmental Management, 184: 85-93. https://doi.org/10.1016/j.jenvman.2016.08.070

[44] Chahinez, H., Abdelkader, O., Leila, Y., Tran, H. (2020). One-stage preparation of palm petiole-derived biochar: Characterization and application for adsorption of crystal violet dye in water. Environmental Technology and Innovation, 19: 100872. https://doi.org/10.1016/j.eti.2020.100872

[45] Aftab, Z.E., Aslam, W., Aftab, A., Shah, A.N., Akhter, A., Fakhar, U., Siddiqui, I., Ahmed, W., Majid, F., Wróbel, J., Ali, M.D., Aftab, M., Ahmed, M.A.A., Kalaji, H.M., Abbas, A., Khalid, U. (2022). Incorporation of engineered nanoparticles of biochar and fly ash against bacterial leaf spot of pepper. Scientific Reports, 12(1): 8561. https://doi.org/10.1038/s41598-022-10795-8

[46] Bolan, N., Sarmah, A.K., Bordoloi, S., Bolan, S., Padhye, L.P., Van Zwieten L., Sooriyakumar, P., Khan, B.A., Ahmad, M., Solaiman, Z.M., Rinklebe, J., Wang, H., Singh, B.P., Siddique, K.H. (2023). Soil acidification and the liming potential of biochar. Environmental Pollution, 317: 120632. https://doi.org/10.1016/j.envpol.2022.120632

[47] Wang, X., Ma, S., Wang, X., Cheng, T., Dong, J., Feng K. (2022). The mechanism of Cu^{2+} sorption by rice straw biochar and its sorption-desorption capacity to Cu^{2+} in soil. Bulletin of Environmental Contamination and Toxicology, 109(3): 562-570. https://doi.org/10.1007/s00128-022-03538-y

[48] Altıkat, A., Alma, M.H., Altıkat, A., Bilgili, M.E., Altıkat, S. (2024). A comprehensive study of biochar yield and quality concerning pyrolysis conditions: A multifaceted approach. Sustainability, 16(2): 937. https://doi.org/10.3390/su16020937

[49] Eldeeb, T.M., Aigbe, U.O., Ukhurebor, K.E., Onyancha, R.B., El-Nemr, M.A., Hassaan, M.A., Ragab, S., Osibote, O. A., El Nemr, A. (2024). Adsorption of methylene blue (MB) dye on ozone, purified and sonicated sawdust biochars. Biomass Conversion and Biorefinery, 14: 9361-9383. https://doi.org/10.1007/s13399-022-03015-w

[50] Munawaroh, F., Muharrami, L.K., Arifin, Z. (2019). Synthesis and characterization of precipitated $CaCO_3$ from ankerite prepared by bubbling method. KnE Engineering, 1(2): 98-104. https://doi.org/10.18502/keg.v1i2.4435

[51] Harizanova, R., Gaydarov, V., Gugov, I., Zamfirova, G., Mihailova, I., Pernikov, M., Rüssel, C. (2023). IR-spectroscopy, thermophysical and mechanical properties of glasses in the system $Na_2O/BaO/TiO_2/B_2O_3/SiO_2/Al_2O_3$. Journal of Chemical Technology and Metallurgy, 58(3): 456-466. https://doi.org/10.59957/jctm.v58i3.74

[52] Shi, Q., Zhang, H., Shahab, A., Zeng, H., Zeng, H., Bacha, A., Nabi, I., Siddique, J., Ullah, H. (2021). Efficient performance of magnesium oxide loaded biochar for the significant removal of Pb^{2+} and Cd^{2+} from aqueous solution. Ecotoxicology and Environmental Safety, 221: 112426. https://doi.org/10.1016/j.ecoenv.2021.112426

[53] Jetsrisuparb, K., Jeejaila, T., Saengthip, C., Kasemsiri, P., Ngernyen, Y., Chindaprasirt, P., Knijnenburg, J.T.N. (2022). Tailoring the phosphorus release from biochar-based fertilizers: role of magnesium or calcium addition during co-pyrolysis. RSC Advances, 12: 30539-30548. https://doi.org/10.1039/D2RA05848K

[54] Chaudhari, S.Y., Rajput, D.S., Galib, R., Prajapati, P.K. (1015). Fourier transform infrared analysis of Tamra Bhasma at different levels: A preliminary study. Ayu, 36(1): 77-82. https://doi.org/10.4103/0974-8520.169013

[55] Rahmat, A., Sutiharni, S., Elfina, Y., Yusnaini, Y., Latuponu, H., Minah, F.N., Sulistyowati, Y., Mutolib, A. (2023). Characteristics of tamarind seed biochar at different pyrolysis temperatures as waste management strategy: Experiments and bibliometric analysis. Indonesian Journal of Science and Technology, 8(3): 517-538. https://doi.org/10.17509/ijost.v8i3.63500

[56] Garcia-Maraver, A., Salvachúa, D., Martínez, M., Diaz, L., Zamorano, M. (2013). Analysis of the relation between the cellulose, hemicellulose and lignin content and the thermal behavior of residual biomass from olive trees. Waste Management, 33: 2245-2249.

[57] Shafiq, M., Capareda, S.C. (2021). Effect of different temperatures on the properties of pyrolysis products of Parthenium hysterophorus. Journal of Saudi Chemical Society, 25(3): 101197. https://doi.org/10.1016/j.jscs.2021.101197

[58] Liu Y, Weng, Z., Han, B., Guo, Z., Tian, H., Tang, Y., Cai, Y., Yang, Z. (2023). Recent studies on the comprehensive application of biochar in multiple environmental fields. Journal of Cleaner Production, 421: 138495. https://doi.org/10.1016/j.jclepro.2023.138495

[59] Adekanye, T., Dada, O., Kolapo, J. (2022). Pyrolysis of maize cob at different temperatures for biochar production: Proximate, ultimate and spectroscopic characterization. Research in Agricultural Engineering, 68(1): 27-34. https://doi.org/10.17221/106/2020-RAE

[60] Ok, Y.S., Yang, J.E., Zhang, Y.S., Kim, S.J., Chung, D.Y. (2007). Heavy metal adsorption by a formulated zeolite-Portland cement mixture. Journal of Hazardous Materials, 147(1-2): 91-96.

[61] Suliman, W., Harsh, J.B., Abu-Lail, N.I, Fortuna, A.M., Dallmeyer, I., Garcia-Perez, M. (2016). Influence of feedstock source and pyrolysis temperature on biochar bulk and surface properties. Biomass and Bioenergy, 84: 37-48. https://doi.org/10.1016/j.biombioe.2015.11.010

[62] Hadi, A.R.A., Norazlina, A.S. (2021). The effects of pyrolysis temperature on chemical properties of empty fruit bunch and palm kernel shell biochars. Earth and Environmental Science, 757: 012029. https://doi.org/10.1088/1755-1315/757/1/012029

[63] Tan, Z., Liu, L., Zhang, L., Huang, Q. (2017). Mechanistic study of the influence of pyrolysis conditions on potassium speciation in biochar "preparation-application" process. Science of the Total Environment, 599: 207-216. https://doi.org/10.1016/j.scitotenv.2017.04.235

[64] Zhang, H., Voroney, R.P., Price, G.W. (2015). Effects of temperature and processing conditions on biochar chemical properties and their influence on soil C and N transformations. Soil Biology and Biochemistry, 83: 19-28. https://doi.org/10.1016/j.soilbio.2015.01.006

[65] Dissanayaka, D.M.N.S., Udumann, S.S., Nuwarapaksha, T.D., Atapattu, A.J. (2023). Effects of pyrolysis temperature on chemical composition of coconut-husk biochar for agricultural applications: A characterization study. Technology in Agronomy, 3(13): 1-8. https://doi.org/10.48130/TIA-2023-0013

[66] Xin, Y., Wang, D., Li, X.Q., Yuan, Q., Cao, H. (2018). Influence of moisture content on cattle manure char properties and its potential for hydrogen rich gas production. Journal of Analytical and Applied Pyrolysis, 130: 224-232. https://doi.org/10.1016/j.jaap.2018.01.005

[67] Yuan, J.H., Xu, R.K., Zhang, H. (2011). The forms of alkalis in the biochar produced from crop residues at different temperatures. Bioresource Technology, 102(3): 3488-3497. https://doi.org/10.1016/j.biortech.2010.11.018

[68] Lee, J.W., Hawkins, B., Day, D.M., Reicosky, D.C. (2010). Sustainability: The capacity of smokeless biomass pyrolysis for energy production, global carbon capture and sequestration. Energy & Environmental Science, 3(11): 1695-1705. https://doi.org/10.1039/C004561F

[69] Lehmann, J., Hansel, C.M., Kaiser, C., Kleber, M., Maher, K., Manzoni, S., Nunan, N., Reichsteinm, M., Schimel, J.P., Torn, M.S., Wieder, W.R., Kögel-Knabner, I. (2020). Persistence of soil organic carbon caused by functional complexity. Nature Geoscience, 13(8): 529-534. https://doi.org/10.1038/s41561-020-0612-3

[70] Smith, P. (2016). Soil carbon sequestration and biochar as negative emission technologies. Global Change Biology, 22(3): 1315-1324. https://doi.org/10.1111/gcb.13178

[71] Woolf, D., Amonette, J.E., Street-Perrott, F.A., Lehmann, J., Joseph, S. (2010). Sustainable biochar to mitigate global climate change. Nature Communications, 1(1): 56. https://doi.org/10.1038/ncomms1053

[72] Sollins, P., Robertson, G.P., Uehara, G. (1988). Nutrient mobility in variable-and permanent-charge soils. Biogeochemistry, 6: 181-199. https://doi.org/10.1007/BF02182995

[73] Mengel, K., Kirkby, E.A. (2001). Principles of Plant Nutrition (5th ed.). Dordrecht: Kluwer Academic Publishers.
[74] Leng, L., Xiong, Q., Yang, L., Li, H., Zhou, Y., Zhang, W., Jiang, S., Li, H., Huang, H. (2021). An overview on engineering the surface area and porosity of biochar. Science of the total Environment, 763(144204): 1-16. https://doi.org/10.1016/j.scitotenv.2020.144204
[75] Ghosh, D., Maiti, S.K. (2021). Effect of invasive weed biochar amendment on soil enzymatic activity and respiration of coal mine spoil: A laboratory experiment study. Biochar, 3: 519-533. https://doi.org/10.1007/s42773-021-00109-y